Volume 1 | Number 1 | Jan 2013 | Pages 1–100

Nanoscale

www.rsc.org/nanoscale

ROYAL SOCIETY
OF CHEMISTRY

ROYAL SOCIETY
OF CHEMISTRY

www.rsc.org/nanoscale

Nanoscale

ARTICLE TYPE

Controllable fabrication of ultrafine oblique organic nanowire arrays and their application on energy harvesting

Lu Zhang,‡[a] Li Cheng,‡[a] Suo Bai,[a,b] Chen Su,[a] Xiaobo Chen,[a] and Yong Qin,[a,b],*

Ultrafine organic nanowire arrays (ONWAs) with controlled direction were successfully fabricated by a novel one-step Faraday cage assisted plasma etching method. The mechanism formation of nanowire arrays was proposed, the obliquity and aspect ratio can be accurately controlled from approximate 0° to 90° via adjusting the angle of sample and etching time, respectively. In addition, the ONWAs were further utilized to improve the output of the triboelectric nanogenerator (TENG). Compared with the
10 **output of TENG composed of vertical ONWAs, the open-circuit voltage, short-circuit current and inductive charges were improved by 73%, 150% and 98%, respectively. This research provides a convenient and practical method to fabricate ONWAs with various obliquities on different materials, which can be used for energy harvesting.**

Introduction

Along with the rapid development of nanotechnologies in
15 recent years, organic nanowires (NWs) as a promising building block for fabricating smart nanodevices, have been extensively applied in organic light-emitting diodes,[1] organic solar cells,[2] field effect transistors,[3] sensors,[4,5] and supercapacitors[6] due to their excellent physical properties and ingenious surface
20 features.[7,8] Organic nanowire arrays (ONWAs) with controlled orientation have shown excellent performance on many aspects in contrast with the random and misalignment structures.[9] Their unique anisotropic properties have been widely applied in microfluidic devices,[10] self-cleaning surface,[11] object transport,[12]
25 dry adhesive[13] and reflection gating.[14] Broadly speaking, ONWAs can be divided into three types: vertical ONWAs, horizontal ONWAs and oblique ONWAs. In previous works, vertical ONWAs have been fabricated through different conventional approaches including block copolymer self-
30 assembly,[15] plasma etching[16,17] and replica molding technique.[18-21] On the other hand, horizontal ONWAs have also been made via various methods such as template free deposition,[22] nanoimprint lithography[23,24] and wrinkling method.[25] Compared with the two types above, although a few approaches have been explored for
35 fabricating oblique ONWAs, the fabrication of oblique ONWAs, especially the ultrafine ONWAs with controllable direction, is still very difficult. For instance, conventional inclined lithography can be employed to fabricate well-defined oblique micropillars distributed uniformly[26] but the refraction and wavelength of
40 incident light limit the angle of inclination and the aspect ratio (AR). In addition, although the mask-assisted low energy ion milling method can realize the obliquity of uniform ONWAs varied from 10° to 40°,[12] but the variation range is small and its formation mechanism decided its low AR. Furthermore, though
45 the ONWAs fabricated by oblique angle polymerization can

possess high AR,[27,28] but the obliquity can't be controlled easily and the density is too high to identify the profile of every NWs. Hence, by now, it is a challenge and high desirable to controllably fabricate high quality oblique ONWAs with high AR
50 in large scale.

In this paper, we reported a novel one-step Faraday cage assisted plasma etching method for the controllable fabrication of ultrafine oblique ONWAs with high AR in large scale. Moreover, we studied the formation mechanism of the oblique ONWAs. In
55 the fabrication process, the moving direction of ions was controlled by the Faraday cage and the ions bombarded on the samples obliquely. The obliquity of ONWAs can be accurately controlled by adjusting the slope of the samples from 0° to 90°, and the length of ONWAs can be simply controlled via adjusting
60 the etching time. By using their anisotropic mechanical property and high AR, the output performance of a triboelectric nanogenerator (TENG) composed of ONWAs was greatly improved. Experimental result shows the open-circuit voltage of the TENG composed of oblique ONWAs (OTENG) was 73%
65 larger than that of the TENG composed of vertical ONWAs (VTENG). And the short-circuit current is also 1.5 times larger.

Results and Discussion

The oblique ONWAs were fabricated by direct reactive ion etching (RIE) without nanopatterns or prefabricated masks. As
70 Figure 1a shows, a cleaning polymer film was put obliquely on the bottom electrode of the RIE machine with an angle α with respect to the electrode, and a Faraday cage consisting of Cu grid top plane and Cu sidewall was covered over the film. The ONWAs were then formed after etching the polymer film under
75 certain experimental parameters (details of the fabrication process are shown in the experimental section). Figure 1b shows a side view scanning electron microscope (SEM) of the fabricated oblique polyethylene terephthalate (PET) NWs array after 70
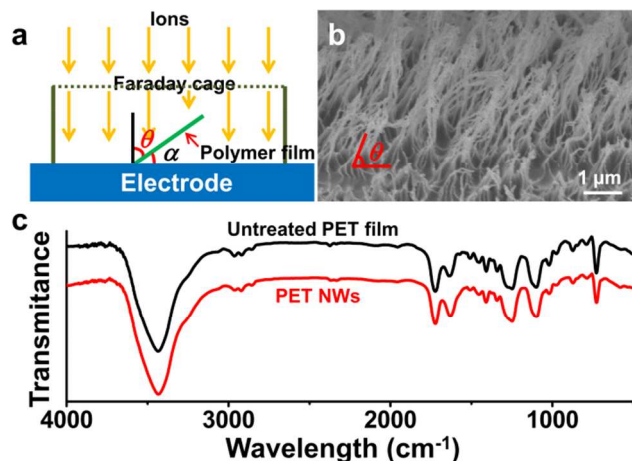
Fig. 1 Fabrication schematic of the oblique ONWAs. (a) Schematic diagram of the fabrication equipment. (b) Side view SEM image of oblique PET NW arrays with the angle θ of 70°. (c) FTIR spectra of untreated PET film and PET NWs taken from a PET NW arrays.

minutes etching. It can be seen that the NWs with about 30 nm in diameter and 2.3 µm in length (aspect ratio = 76) distributed uniformly on PET film, the angle θ between the nanowires and the PET film surface is about 70°, which is the coangle of the
5 angle α. Figure 1c shows the Fourier transform infrared (FTIR) spectra of an untreated PET film and PET NWs fabricated in this method. There is no obvious difference between the two spectra, indicating the ONWAs have the same chemical composition with PET film. Hence, ultrafine ONWAs with controlled direction can
10 be in-situ fabricated from the polymer sheet and have the same composition with the substrate.

In previous works, surface roughness or initial bumps formed on the polymer surface are explained as the reasons for the formation mechanism of ONWAs fabricated by plasma etching.[17,
15 29] In this work, we propose a new mechanism for the formation of ONWAs based on experimental results. As shown in Figure 2a, the fabrication process can be divided into two stages. First, a part of ions bombarded on the surfaces of the steel electrode and Cu grid during the accelerating path, which led to metal particles
20 such as Cu, Fe, Cr, Mn and Zn sputtering off and depositing on the polymer surface. Meanwhile, a part of the metal particles could be oxidized in the oxygen atmosphere, and then the metal or metal oxide particles formed a mask on the surface and prevented the below polymer film from etching. Second, the ions
25 passed through the Faraday cage and bombarded on the polymer with an angle θ with respect to the film surface. During the fabrication process, the Faraday cage can control the moving direction of ions and further control the direction of the ONWAs in-situ appeared on the film for the following mechanism. When
30 a Faraday cage is employed in the plasma atmosphere, a plasma sheath forms on the exterior surface of the Faraday cage, which leads to the zero electric field inside the cage. Therefore, the ions can be accelerated in electric field and pass through the hollows of the grid with the normal direction to the electrode plane. On
35 the contrary, without the Faraday cage, the plasma sheath forms on the surface of substrate and the accelerated ions directly bombard on the substrate surface along its normal direction.[13, 30] This implies that the angle of oblique etching can be easily controlled by adjusting the angle α of the substrate covered by a
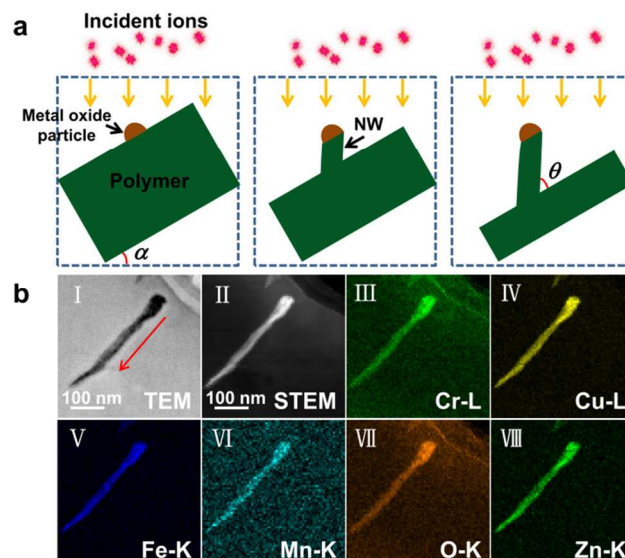
Fig. 2 Formation mechanism of the oblique ONWAs. (a) Schematic image of the fabrication process. (b) BFTEM image (Ⅰ), STEM image (Ⅱ), and EDX mapping images (Ⅲ-Ⅷ) of a single PET NW taken from the PET NW array. The red arrow represents the orientation of the NW from the top to the bottom.

40 Faraday cage. Therefore, the part of polymer film without metal or metal oxide particles' protection was etched by the ions quickly, and oblique ONWAs with an angle θ gradually formed on the surface of film. In order to check the mechanism proposed above, we tested the distribution of elements on the surface of
45 NWs. Figure 2b shows the bright field transmission electron microscopy (BFTEM) image, scanning transmission electron microscopy (STEM) image and energy dispersive X-Ray spectroscopy mapping (EDX mapping) images of Cu, Fe, Cr, Mn, Zn and O of a single PET NW. It is clear that all the elements of
50 Cu, Fe, Cr, Mn, Zn and O have much higher concentration at the top of the NW and these metal elements are just the major composition of the steel electrode and Cu grid, which further proves the above mechanism that the metal or metal oxide particles act as a mask in the etching process.

55 As the tilt angle of the polymer film can be accurately controlled in our experiment, the incident angle of ions with respect to the substrate could be controlled as well. Hence, the
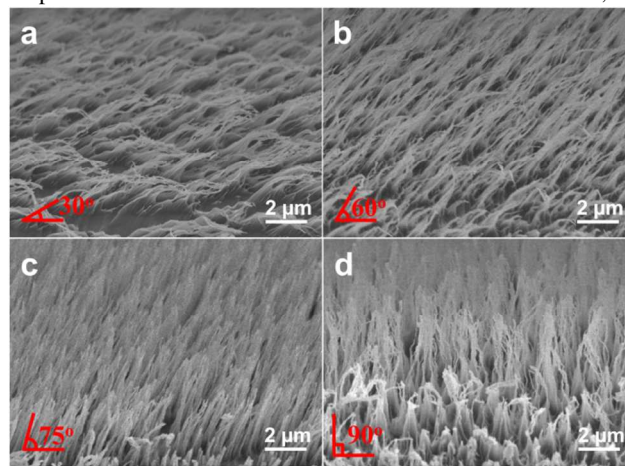
Fig. 3 PET NW arrays with precisely controlled obliquity. (a-d) show the section view SEM images of PET NW arrays with the angle of 30° (a), 60° (b), 70° (c) and 90° (d), respectively.
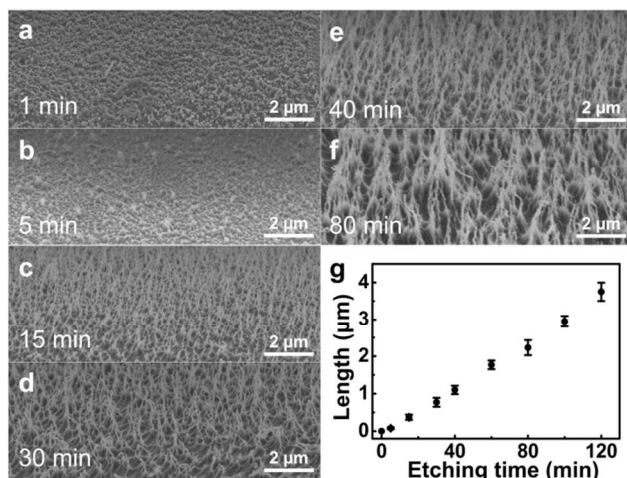
Fig. 4 Length of PET NW arrays changes with different etching times. (a-f) show the section view SEM images of oblique PET NW arrays after 1 (a), 5 (b), 15 (c), 30 (d), 40 (e) and 80 (f) minutes etching. (g) shows a nearly linear relationship between the etching time and the PET NWs' length.

ONWAs with different obliquity on films can be fabricated by changing the tilt angle of the polymer film. In the experiment, we fabricated oblique PET NW arrays by placing the PET film with the angle α of 60°, 30°, 15° and 0°. The section view SEM

5   images shown in Figure 3 demonstrate that the PET ONWAs with different obliquities 30°, 60°, 75° and 90°, which have the similar size about 2 µm in length, 30 nm in diameter after 60 minutes etching. This result indicates that the obliquity of the ONWAs can be accurately controlled in a wide range using this

10   method. In addition, the size of ONWAs with different obliquities keeps almost the same.

Additionally, the ONWAs' length can be controlled easily by changing the etching time. Because of the metal or metal oxide mask existing on the top of the NWs to protect the polymer below

15   in the whole fabrication process, the length of the NWs could grow continuously with the increasing etching time. Figures 4a-f show the SEM images of PET NWs after 1, 5, 15, 30, 40 and 80 minutes etching, respectively. Furthermore, a nearly linear relationship between the length of PET NWs and etching time is

20   observed as shown in Figure 4g, which means the oblique NW's length can be accurately controlled by simply adjusting the etching time.

A series of further experiments have been conducted to study whether the oblique ONWAs could be fabricated on any other

25   polymers through this method. In the experiment, different substrates were located with an angle of 45° with respect to the electrode covered over by a Faraday cage. Figures 5a-d demonstrate the SEM images of oblique ONWAs fabricated on polyimide (Kapton) film, poly-p-phenylene terephthamide

30   (Kevlar) fiber, carbon fiber and polypropylene (PP) fiber. The corresponding diameters are about 69, 42, 33 and 73 nm, respectively. This result reveals the wide versatility of this method. Using this novel one-step Faraday cage assisted plasma etching method, the oblique ONWAs of different materials can be

35   fabricated on different kinds of substrates.

Oblique ONWAs have been widely employed in different areas due to their unique anisotropic properties. Nowadays, TENG is a new kind of device that can convert mechanical
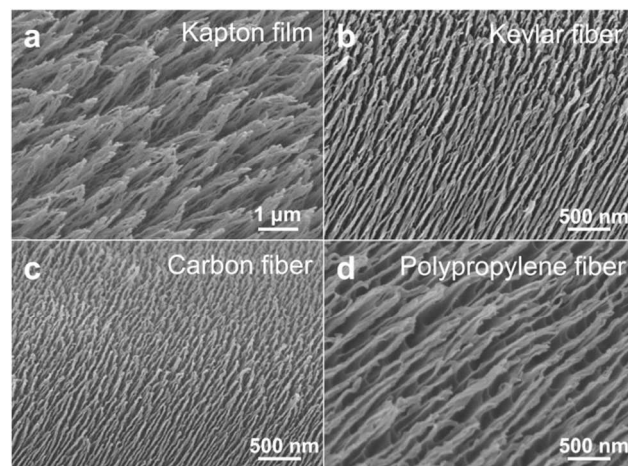
Fig. 5 SEM images of oblique ONWAs fabricated on various substrates. (a) Kapton film, (b) Kevlar fiber, (c) Carbon fiber, (d) PP fiber.

energy existing in the environment to electric energy. The

40   working principle of this TENG can be explained by the combination of triboelectric effect and electrostatic effect, which has been discussed clearly in previous works.[31, 32] The TENG's performance is mainly determined by the materials' ability to gain or lose electrons and the structure of the device, and making

45   micro/nano structures is another important way to improve a TENG's performance.[31-36] With better designed nanostructures, the performance of TENG could be further improved. As shown in Figure 6a, a typical arch-shaped TENG[37] was composed of two kinds of materials with different tendencies to gain or lose

50   electrons. The materials selected here are Kapton film with oblique ONWAs and polyamide (nylon) film spin-coated on the Kapton film (details of the fabrication process are shown in the experimental section). Previous study has reported that applying the vertical ONWAs on the TENG can improve the electric

55   output of the device due to the enhanced surface roughness.[31] As the partial enlarged view of arch-shaped TENG is shown in
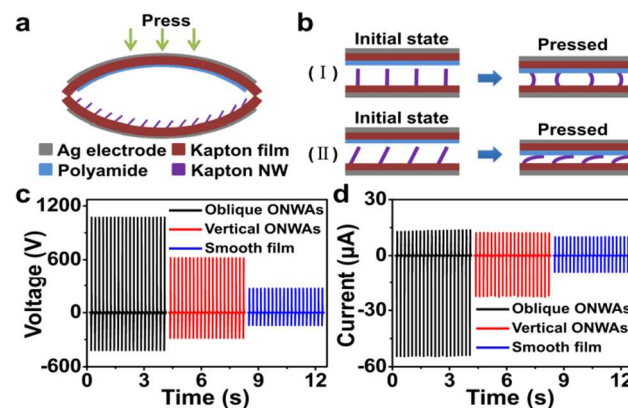
Fig. 6 A TENG composed of oblique ONWAs. (a) Schematic image of an arch-shaped TENG. (b) Schematic diagram of the possible friction movements of the vertical NWs (□) and oblique NWs (□). When the two substrates are brought into contact, oblique NWs are easier to bend and slide on the surface of Kapton film to enhance the friction. (c,d) Comparison of the open-circuit voltage (c) and short-circuit current (d) of TENGs composed of oblique ONWAs, vertical ONWAs and smooth film, respectively.

Figure 6B, by replacing the vertical ONWAs with oblique ONWAs, it can be seen that the oblique NWs are easier to bend and slide on the surface of Kapton film when the two substrates are brought into contact, which can enlarge the additional friction and produce much more triboelectric charges on the surface of electrodes.[38] Based on that assumption, the performance of the TENG is expected to be largely improved. Figure 6c and d show that the open-circuit voltages of the OTENG, the VTENG and the TENG composed of smooth film (STENG) are 1070 V, 620 V, 265 V, and the short-circuit currents are 55 µA, 22 µA and 9 µA. In addition, the corresponding inductive charges of these TENGs are 103 nC, 52 nC and 22 nC. Compared with the electric output of the STENG, the open-circuit voltage, short-circuit current and inductive charges of the VTENG increased 134%, 144% and 136%, respectively. This enhanced performance was due to the improved surface roughness introduced by the vertical ONWAs. And this improvement can provide additional friction and generate more triboelectric charges.[31] Furthermore, compared with the electric output of the VTENG, the open-circuit voltage, short-circuit current and inductive charges of OTENG were improved by 73%, 150% and 98%, respectively. The enhancement corresponded well with the assumption that the oblique NWs are easier to bend and slide on the surface of the Kapton film which lead to the enhancement of the additional friction and generate much more triboelectric charges. These results demonstrate that oblique ONWAs are effective in increasing the output energy of a TENG.

Conclusions

In summary, we developed a novel one-step Faraday cage assisted plasma etching method for fabrication of ultrafine oblique ONWAs with the merit of high AR in large scale and precisely controlled obliquity and length. The formation of the ONWAs is due to the formation of sputter-induced metal or metal oxidation mask and the mask-protected etching process. In addition, the oblique ONWAs were employed to improve the output of the TENG. Compared with the output of TENG composed of vertical ONWAs, the open-circuit voltage, short-circuit current and inductive charges were improved by 73%, 150% and 98%, respectively. This fabrication technique laied a solid foundation for the oblique ONWAs' potential applications including energy conversion, microelectronics, chemical and biological sensing.

Experimental Section

Fabrication of oblique ONWAs on the surface of PET films

A PET film was first ultrasonic cleaned by acetone, ethanol and deionized water for 15 minutes successively, and then the film was blow-dried. Subsequently, the film was obliquely placed on the electrode of the RIE machine with an angle α and then covered over by a Faraday cage consisting of copper grid top plane and Cu sidewall, the top plane of the Faraday cage was paralleled with the electrode. The diameter and the height of the Faraday cage employed in our experiment are 180 mm and 35 mm, respectively. After vacuumized the chamber of RIE machine to 4×10^{-4} Pa, the film was etched with 60 sccm O_2 flow ratio, 2 Pa pressure, 100 W input power, and 400 V automatic bias.

Fabrication of the TENG

Two pieces of 230 µm thick Kapton film (4.5 cm × 4.5 cm in size) were first cleaned by acetone, ethanol and deionized water for 15 minutes successively, and then the film was blow-dried. Then an Ag electrode was sputtered on the convex surface of each Kapton film. Oblique NW array was then fabricated on the concave surface of one piece of the Kapton film, the angle α was 30°, and etching time was 60 minutes. This film was subsequently immersed in 2 M hydrochloric acid solution for 30 minutes to remove the metal or metal oxide particles on the surface of NWs and then washed with deionized water. The nylon solution was prepared by mixing with formic acid and polyamide in a rate of 3:7 (w/w) and then a thin film of nylon solution was spin-coated on the concave surface of the other piece of Kapton film with the speed of 2000 rpm for 30 s. The two pieces of films were then dried in an oven at 80 °C for 30 minutes and sealed together with the ONWAs facing with the nylon film. The maximum distance between the two electrodes of the arch-shaped OTENG is about 15 mm. The VTENG and STENG have the same fabrication process with OTENG, except that the Kapton film with oblique NWs is replaced by Kapton film with vertical NWs and smooth Kapton film without treatment, respectively.

Notes and references

[a] Institute of Nanoscience and Nanotechnology, School of Physical Science and Technology, Lanzhou University, Lanzhou, 730000, China.
E-mail: qinyong @lzu.edu.cn
[b] The Research Institute of Biomedical Nanotechnology, Lanzhou University, Lanzhou, 730000, China.
† Electronic Supplementary Information (ESI) available. See DOI:10.1039/b000000x/
‡ These authors contributed equally to this work.

1   R. J. Tseng, J. X. Huang, J. Ouyang, R. B. Kaner, Y. Yang, *Nano Lett.*, 2005, **5**, 1077.
2   M. Law, L. E. Greene, J. C. Johnson, R. Saykally, P. D. Yang, *Nat. Mater.*, 2005, **4**, 455.
3   J. A. Merlo, C. D. Frisbie, *J. Phys. Chem. B*, 2004, **108**, 19169.
4   Y. Chen, Y. Luo, *Adv. Mater.*, 2009, **21**, 2040.
5   K. Wang, J. Huang, Z. Wei, *J. Phys. Chem. C*, 2010, **114**, 8062.
6   H. D. Tran, D. Li, R. B. Kaner, *Adv. Mater.*, 2009, **21**, 1487.
7   A. K. Wanekaya, Y. Lei, E. Bekyarova, W. Chen, R. Haddon, A. Mulchandani, N. V. Myung, *Electroanalysis*, 2006, **18**, 1047.
8   L. Liang, J. Liu, C. F. Windisch, G. J. Exarhos, Y. H. Lin, *Angew. Chem.-Int. Edit.*, 2002, **41**, 3665.
9   H. Sato, D. Yagyu, S. Ito, S. Shoji, *Sens. Actuator A-Phys.*, 2006, **128**, 183.
10   Y. Zheng, X. Gao, L. Jiang, *Soft Matter*, 2007, **3**, 178.

11   W. Wu, L. Cheng, S. Bai, Z. L. Wang, Y. Qin, *Adv. Mater.*, 2012, **24**, 817.

12   H. E. Jeong, J. K. Lee, H. N. Kim, S. H. Moon, K. Y. Suh, *Proc. Natl. Acad. Sci. U. S. A.*, 2009, **106**, 5639.

5 13   L. Cheng, W. Dou, S. Bai, W. Wu, Q. Xu, Y. Qin, *Sci. Adv. Mater.*, 2013, **5**, 1179.

14   A. K. Khandpur, S. Forster, F. S. Bates, I. W. Hamley, A. J. Ryan, W. Bras, K. Almdal, K. Mortensen, *Macromolecules*, 1995, **28**, 8796.

10 15   H. Fang, W. Wu, J. Song, Z. L. Wang, *J. Phys. Chem. C*, 2009, **113**, 16571.

16   E. Wohlfart, J. P. Fernandez-Blazquez, E. Knoche, A. Bello, E. Perez, E. Arzt, A. del Campo, *Macromolecules*, 2010, **43**, 9908.

17   Y. N. Xia, G. M. Whitesides, *Annu. Rev. Mater. Sci.*, 1998, **28**, 153.

15

18   J. L. Wilbur, A. Kumar, H. A. Biebuyck, E. Kim, G. M. Whitesides, *Nanotechnology*, 1996, **7**, 452.

19   Y. N. Xia, E. Kim, G. M. Whitesides, *Chem. Mat.*, 1996, **8**, 1558.

20   L. J. Guo, *Adv. Mater.*, 2007, **19**, 495.

20 21   C. Liu, K. Hayashi, K. Toko, *Macromolecules*, 2011, **44**, 2212.

22   S. Y. Chou, P. R. Krauss, W. Zhang, L. J. Guo, L. Zhuang, *J. Vac. Sci. Technol. B*, 1997, **15**, 2897.

23   S. Y. Chou, P. R. Krauss, P. J. Renstrom, *J. Vac. Sci. Technol. B*, 1996, **14**, 4129.

25 24   C. M. Stafford, B. D. Vogt, C. Harrison, D. Julthongpiput, R. Huang, *Macromolecules*, 2006, **39**, 5095.

25   C. Beuret, G. A. Racine, J. Gobet, R. Luthier, N. F. de Rooij, presented at Proceedings of the IEEE Workshop on Micro Electro Mechanical Systems 1994 .

30 26   S. Pursel, M. W. Horn, M. C. Demirel, A. Lakhtakia, *Polymer*, 2005, **46**, 9544.

27   M. C. Demirel, S. Boduroglu, M. Cetinkaya, A. Lakhtakia, *Langmuir*, 2007, **23**, 5861.

28   J. R. Morber, X. Wang, J. Liu, R. L. Snyder, Z. L. Wang, *Adv. Mater.*, 2009, **21**, 2072.

35

29   B. O. Cho, S. W. Hwang, J. H. Ryu, S. H. Moon, *Rev. Sci. Instrum.*, 1999, **70**, 2458.

30   G. Zhu, C. Pan, W. Guo, C. Y. Chen, Y. Zhou, R. Yu, Z. L. Wang, *Nano Lett.*, 2012, **12**, 4960.

40 31   F. R. Fan, L. Lin, G. Zhu, W. Wu, R. Zhang, Z. L. Wang, *Nano Lett.*, 2012, **12**, 3109.

32   N. Vu, R. Yang, *Nano Energy*, 2013, **2**, 604.

33   Y. Yang, H. Zhang, Z. L. Wang, *Adv. Funct. Mater.*, 2014, **24**, 3745.

45 34   P. Bai, G. Zhu, Z. H. Lin, Q. Jing, J. Chen, G. Zhang, J. Ma, Z. L. Wang, *Acs Nano*, 2013, **7**, 3713.

35   F. R. Fan, Z. Q. Tian, Z. L. Wang, *Nano Energy*, 2012, **1**, 328.

36   G. S. P. Castle, *J. Electrost.*, 1997, **40-41**, 13.

Nanoscale Accepted Manuscript